Langmuir

ARTICLE

pubs.acs.org/Langmuir

Polyaniline Nanoscaffolds for Colorimetric Sensing of Biomolecules via Electron Transfer Process

M. Jinish Antony[†] and M. Jayakannan[*,‡]

[†]Chemical Sciences and Technology Division, National Institute for Interdisciplinary Science and Technology, Thiruvananthapuram 695019, Kerala, India

[‡]Department of Chemistry, Indian Institute of Science Education and Research (IISER), 900, NCL Innovation Park, Dr. Homi Bhabha Road, Pune − 411 008, Maharashtra, India

Supporting Information

ABSTRACT: Biologically important analytes such as cysteine and vitamin-C were detected by electron transfer (ET) via naked eye colorimetric sensing using a tailor-made water-soluble self-doped polyaniline (PSPANa) as a substrate. Monomer (*N*-3-sulfopropylaniline) was synthesized via ring-opening of propane sultone with excess aniline and polymerized in water using ammonium persulfate to obtain green water-soluble polymer. Vitamin-C (ascorbic acid) and cysteine showed unexpected sharp and instantaneous color change from blue to colorless sensing action. The stoichiometry of the analyte to polymer was determined as 3:2 and 4:1 with association (or binding) constants of $K = 2.1 \times 10^3$ and 1.5×10^3 M^{-1} for vitamin-C and cysteine, respectively. Efficient electron transfer from vitamin-C (also cysteine) to the quinoid unit of the polyaniline base occurred in solution; as a result, the color of the solution changed from deep blue to colorless. Cyclic voltammetry analysis of PSPANa showed the disappearance of the cathodic peak at −0.21 V upon the addition of analytes (vitamin-C and cysteine) and confirms the electron transfer from the analyte to the polymer backbone. Dynamic light scattering (DLS) and zeta potential techniques were utilized to trace the molecular interactions in the electron transfer process. DLS histograms of the polymer samples confirmed the existence of nanoaggregates of 8−10 nm in diameter. The polymers possessed typical amphiphilic structure to produce micellar aggregates which facilitate the efficient electron transfer occurred between the analyte and polyaniline backbone.

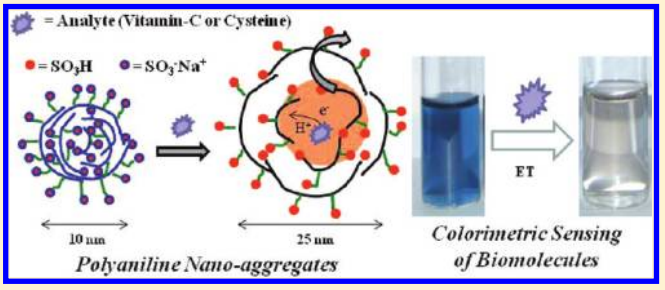

INTRODUCTION

Conducting polymers are emerging as important class of active layers in optoelectronic devices and chemical sensors.[1−4] Polyaniline, polypyrrole, polyphenylenevinylene, polythiophene, and polyflourenes were reported for chemical sensing of biomolecules such as DNA, RNA, enzymes, proteins, nucleic acids, and so on.[5−8] Among all these conjugated polymers, polyaniline is unique due to its good environmental−chemical−thermal stability and excellent reversible non-redox acid/base doping process. The protonation and deprotonation in the polymer backbone is accomplished by both color change as well as solid state conductivity. Electrochemical assays of polyaniline were reported for detecting bioanalytes such as dopamine, glucose, cholesterol, vitamins, and various gases such as HCl, ammonia, H_2S, and hydrogen, and so forth.[9−18] However, the mechanism of the sensing was more difficult to interpret due to the complex surface morphology, and detailed characterization techniques were usually required to confirm the detection pathways.[19−21] Further, poor solubility of polyaniline in water or organic solvents is always an inherent major obstacle in making the assays. To increase the solubility of polyaniline, aryl and N-substituted polyaniline derivatives were synthesized via postpolymerization sulfonation of emeraldine base using fuming sulfuric acid or other substitution reactions.[22−27] Attempts were also reported for self-doped polymers such as N-alkyl sulfonated monomers via electrochemical polymerization.[27] These approaches produced either low molecular weight polymers or insoluble polymers which hampered their complete structural characterization.[28,29] Nanostructures of polyanilines such as nanofibers, nanospheres, and gels were also reported to disperse the nanomaterials in water or organic solvents so that stable films could be prepared for sensor application.[1,2,30] Though the nanostructures showed improved processability, making mechanically stable polyaniline films without losing the morphology or conductivity is still far from the reality. Chemical or biological sensing via colorimetric naked eye detection is an inexpensive technique and also useful for online monitoring in vitro and in vivo studies.[31−34] Polyaniline exists in three major forms: (i) green color emerldine salt, (ii) blue color emeraldine base, and (iii) colorless leucoemerldine base form (completely reduced state with absorbance in the

Received: January 5, 2011
Revised: April 12, 2011
Published: April 25, 2011

UV-region less than 320 nm) in solution.[35,36] The change of the color from blue to colorless is particularly interesting for sensing applications, since it matches with detection capabilities of the human eye. Color change from blue (emeraldine base) to colorless form (leucoemeraldine base) is accompanied by both electron as well as proton transfer. This concept is not explored for sensing of biomolecules mainly due to two important reasons: (i) lack of complete solubility of polyaniline materials in water and (ii) mismatching of the redox potential of analytes with polyaniline backbone. Therefore, developing new approaches for making functionalized and water-soluble polyaniline derivatives and exploring them for colorimetric sensing via naked eye detection is a challenging problem to be addressed for both fundamental understanding as well as developing new systems for sensing of new chemical or biological analytes.

In the present approach, a water-soluble N-substituted self-doped polyaniline, poly-*N*-sulfopropane aniline (PSPA), was synthesized via oxidative solution polymerization route. The polymer was freely soluble in water which enabled its structural characterization by NMR and other spectroscopic techniques. The blue colored sodium salt of the polymer (PSPANa) was employed as substrate for the detection of cysteine and vitamin-C. Dynamic light scattering and zeta potential analysis were utilized to trace the molecular interactions and polymer self-assembly in doped and dedoped forms. It was found that the polymers exist as nanomicellar aggregates of 8−10 nm with surface charges of −20 to −30 mV. The polymer aggregates act as nanoreactor sites for efficient electron transfer (ET) processes. ET was accompanied by an instantaneous sharp change from blue to colorless for naked eye detection of biomolecules. Job's plot was utilized to calculate the stochiometry, and the molar ratio method was employed to calculate association constant of polymer + analyte complex using the Benesi−Hildebrand equation. The mechanism of the electron transfer process was further confirmed by redox potential analysis by cyclic voltammetry. In a nutshell, electron-transfer process was utilized in a self-doped water-soluble polyaniline for naked eye colorimetric sensing of biologically active molecules such as vitamin-C and cysteine.

EXPERIMENTAL SECTION

Materials. Aniline, ammonium persulphate (APS), and propanesultone were purchased from Sigma Aldrich Chemicals. Vitamin-C, sodium hydroxide, sodium carbonate, and hydrochloric acid were purchased from Merck Chemicals (India). All the above chemicals are used without further purification.

Measurements. NMR spectra of the compounds were recorded using a 500 MHz Bruker NMR spectrophotometer in D_2O containing small amount of tetramethylsilane (TMS) as internal standard. Infrared spectra of the polymers were recorded using a Thermo Scientific Nicolet 6700 Fourier transform infrared (FT-IR) spectrometer in the range of 4000−400 cm^{-1}. The purity of the samples were determined by fast atom bombardment high-resolution mass spectrometry (FAB-HRMS: JEOL JSM 600). The molecular weights of the polymers were determined using an Applied Bio Instruments 4800 Plus MALDI-TOF-TOF apparatus. For conductivity measurements, the polymer samples were pressed into a 10 mm diameter pellet and analyzed with a four-probe using a Keithley 6221 DC and AC current source and 2181A nanovoltmeter. The resistivities of the sample were measured at five different positions. Temparature dependent measurement of the polymer samples was carried out with a PID controlled heating oven. For scanning electron microscopy (SEM) measurements, polymer samples were subjected to a thin gold coating using a JEOL JFC-1200 fine coater. The probing side was inserted into a JEOL JSM −5600 LV scanning electron microscope for taking photographs. Transmission electron microscopy (TEM) analysis was conducted using a Tecnai 30 G^2 S-twin 300 KV high-resolution transmission electron microscope. For TEM measurements, a suspension of self-doped material is dispersed in methanol and deposited on a Formvar-coated copper grid via drop by drop addition using a glass dropper. Wide angle X-ray diffraction (WXRD) patterns of the finely powdered polymer samples were recorded with a Philips analytical diffractometer using Cu Kα emission. The spectra were recorded in the range of $2\theta = 0-40$ and analyzed using X'Pert software. The size determination of the polymer solution is carried out by dynamic light scattering (DLS), using a Nano ZS-90 apparatus utilizing 633 nm red laser from Malvern instruments. UV−visible spectra of the polymers were recorded using an Evolution 300 UV−visible instrument from Thermo Scientific Instruments. The pH values of the samples were measured using a pH 1500 pH meter from Eutech Instruments and calibrated using buffer solutions of pH 4, 7, and 12. The thermal stability of the polymers was determined using a PerkinElmer STA 6000 simultaneous thermal analyzer at a heating rate of 10 °C/min in nitrogen. The instrument for thermogravimetric analysis (TGA) was calibrated with calcium oxalate monohydrate as standard. DSC scans of the samples were recorded with a DSC Q 20 apparatus from TA Instruments, at a heating rate of 10 °C/min in nitrogen atmosphere, and the instrument was calibrated using indium standard. Cyclic voltammetry (CV) of the samples was measured by using an Epsilon E2 cyclic voltammeter using Ag/AgCl reference electrode, platinum counter electrode, and glassy carbon working electrode.

Synthesis of *N*-3-Sulfopropylaniline (SPA). Excess aniline (5.0 mL, 0.06 mol) was taken in a 100 mL round-bottom flask, and propane sultone (1.35 g, 0.01 mol) was added dropwise. The solution was stirred at room temperature for 6 h. The resultant white solid was poured into acetone, filtered, and washed with acetone until the filtrate become colorless. The solid was dried under vacuum oven for 12 h at 50 °C. It was further purified by recrystallization from hot methanol. Yield = 8.80 g (95%). ^{1}H NMR (500 MHz, D_2O) δ: 7.46 (m, 3H, Ar−H), 7.36 (d, 2H, Ar−H), 3.47 (t, 2H, NH−C**H**$_2$−), 2.9 (t, 2H, C**H**$_2$−SO_3H), 2.06 (m, 2H, aliphatic-H). ^{13}C NMR (125 MHz, D_2O) δ: 134.5, 130.4, 129.9, 122.3, 50.2, 47.7, 20.9. FT-IR (KBr, cm^{-1}): 1594, 1472, 1168, 1045, 756, 695, 609. FAB-HRMS (MW = 215.06): m/z 214.65 (M^+). Anal. Calcd. for $C_9H_{13}NO_3S$: C, 50.21; H, 6.09. Found: C, 50.31; H, 6.01.

Synthesis of Poly-*N*-3-sulfopropylaniline (PSPA). *N*-3-Sulfopropyl-aniline (1.00 g, 4.70 mmol) was dissolved in water (17.0 mL). APS (1.06 g, 4.70 mmol) in water (3.0 mL) was added to monomer solution at 30 °C, and the polymerization was allowed to proceed for 2 h without disturbance. The green polymer solution was precipitated into acetone, filtered, and washed with acetone until the filtrate became colorless. The green powder was dried in a vacuum oven at 60 °C for 6 h. Yield = 0.85 g (85%). ^{1}H NMR (500 MHz, D_2O) δ: 7.46 (m, 3H, Ar−H), 7.37 (d, 2H, Ar−H), 3.48 (t, 2H, NH−C**H**$_2$−), 2.9 (t, 2H, C**H**$_2$−SO_3H), 2 (t, 2H, aliphatic-H). FT-IR (KBr, cm^{-1}): 1579, 1493, 1401, 1163, 1045, 807, 736, 598, 522. UV−visible (water, nm): 320, 415, 780, 1040.

Synthesis of Sodium Salt of Poly-*N*-3-sulfopropylaniline (PSPANa). Poly-*N*-3-sulfopropyl-aniline (1.00 g) was dissolved in water (1.0 mL) and treated with NaOH solution (1.0 mL, 5 M). The solution was stirred, and the resultant blue colored solution was precipitated from methanol. The blue powder was filtered and dried in vacuum oven 60 °C for 6 h. Yield = 0.95 g (95%). ^{1}H NMR (500 MHz, D_2O) δ: 6.77 (t, 2H, Ar−H), 6.4 (d, 4H, Ar−H), 3.22 (t, 2H, aliphatic), 2.76 (t, 2H, aliphatic), 2.3 (m, 2H, aliphatic). FT-IR (KBr, cm^{-1}): 1620, 1498, 1360, 1168, 1045, 817, 736, 603, 527. UV−visible (water, nm): 300, 630.

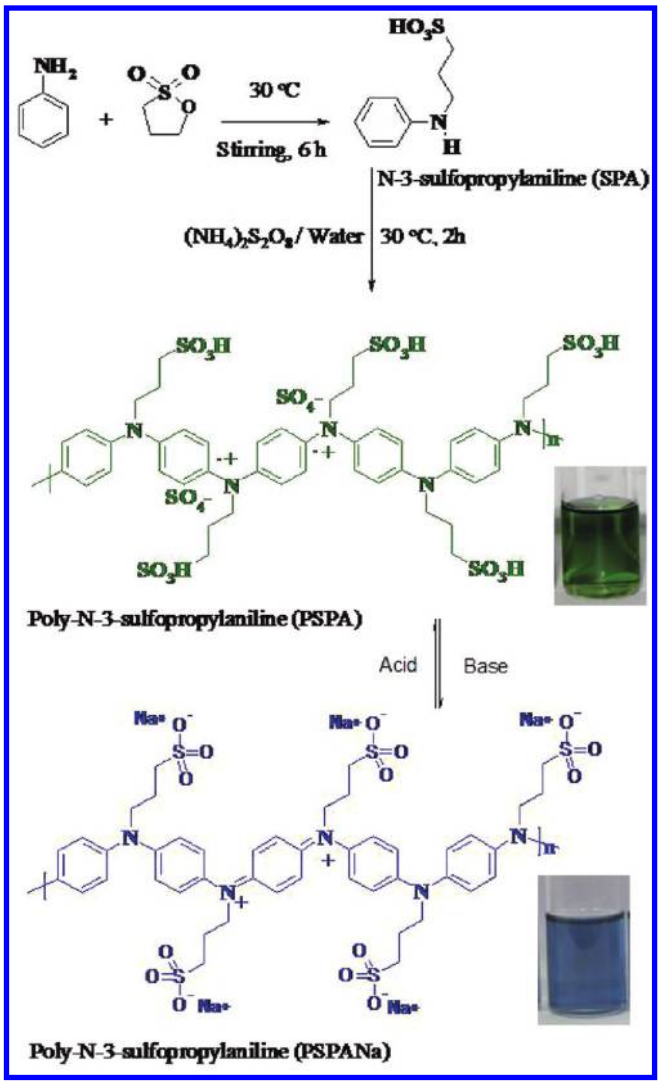

Figure 1. Synthesis of the monomer (SPA) and self-doped polymer PSPA.

RESULTS AND DISCUSSION

The monomer (*N*-3-sulfopropyl aniline) was synthesized via ring-opening of propane sultone with excess aniline and purified by recrystallization from hot methanol (see Figure 1). The monomer was polymerized in water using ammonium persulfate as oxidizing agent, and the resultant polymer, poly-*N*-3-sulfopropyl-aniline (PSPA), was isolated as dark green solid. The emeraldine salt (green solid) was found to be soluble in water and reacted with sodium hydroxide or sodium carbonate to produce deep blue colored polyaniline emeraldine base, poly-N-3-sulfopropyl-aniline sodium salt (PSPANa). Usually, polyanilines are not soluble in water or organic solvents which limited their complete structural characterization.[30] In the present case, polymers in both emeraldine salt and base form have shown good solubility in water which enabled their structural characterization by ^{1}H and ^{13}C NMR. ^{1}H NMR spectra of the monomer and polymers (PSPA and PSPANa) were recorded in D_2O, and the spectra are shown in Figure 2. The peaks at 7.46−7.36 ppm in the monomer were assigned to aromatic protons, and their aliphatic protons appeared at 3.47, 2.9, and 2.06 ppm. The emeraldine salt (PSPA) showed two peaks at 7.46 and 7.37 ppm with respect to

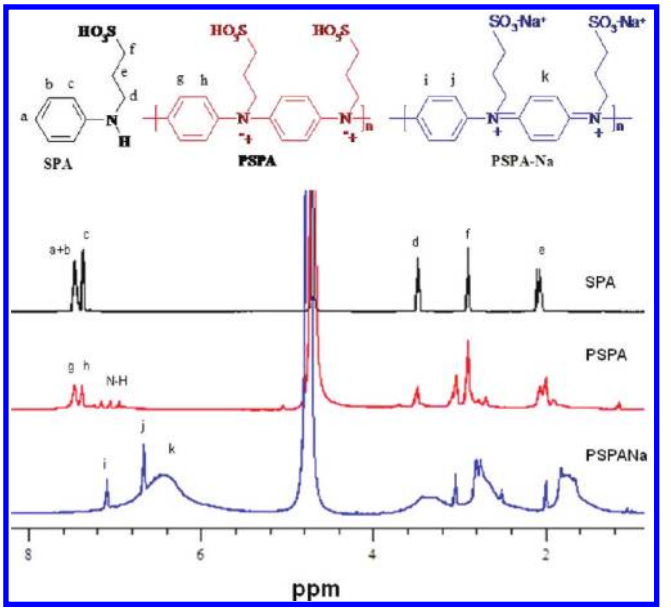

Figure 2. ^{1}H NMR spectra of the monomer (SPA), PSPA, and PSPANa in D_2O.

benzenoid ring aromatic protons. The three equally intense peaks at 7.15/7.05/7.95 with 1:1:1 intensity (J = 50 Hz) were assigned to N−H protons in the conducting self-doped polyaniline. The sodium salt of the polymer (PSPANa) showed large peak shifts compared to PSPA; the peaks corresponding to benzonoid-aromatic peaks were shifted to the upfield region at 7.04 and 6.65 ppm.[37−39] The broad peak that appeared at 6.21−6.63 ppm was assigned to the aromatic protons of quinoid rings in the dedoped form. The disappearance the N−H protons (at 7.15−7.95 ppm) and the appearance of the quionoid-ring protons in the PSPANa directly provided evidence for the formation of dedoped structure. The number and intensity of protons matched with the expected structure of the compounds (see the Supporting Information for SPA). ^{13}C NMR spectra of the monomer, PSPA and PSPANa in D_2O showed peaks with respect to their number of aromatic and aliphatic carbon atoms (see Supporting Information). FT-IR spectra of the monomer, PSPA, and PSPANa were recorded by making thin pellets with KBr (see the Supporting Information). The two strong vibrations in the monomer at 1594 and 1472 cm^{-1} were assigned to symmetric (C═C) and antisymmetric (C═C) stretching. The peaks at 1599 and 1498 cm^{-1} in the polymers were assigned to stretching vibrations of C═C (quinoid) and C═C (benzenoid), respectively.[40−42] The peaks at 1350, 1250, and 1041 cm^{-1} were assigned to C−N, O═S═O, and C−H vibrations, respectively.[30] The inherent viscosity of the polymer was obtained as 0.18 dL/g in water at 30 °C, which indicates the formation of moderate molecular weight polyanilines.[30] To further confirm the formation of polymers, the doped polymer was subjected to MALDI-TOF analysis using α-cyano-4-hydroxy-cinnamic acid as a matrix (see the Supporting Information). The mass spectrum showed peaks at regular intervals of 213 amu corresponding to the repeating units of the polymer chain $P_n = (C_9H_{11}NO_3S)_n$.

The morphology of the PSPA was analyzed by SEM and high-resolution TEM. The SEM images of PSPA confirmed the existence of the flakelike morphology of the polymers in the solid state (see Figure 3). The TEM image of the polymer also

dx.doi.org/10.1021/la200047t |*Langmuir* 2011, 27, 6268–6278

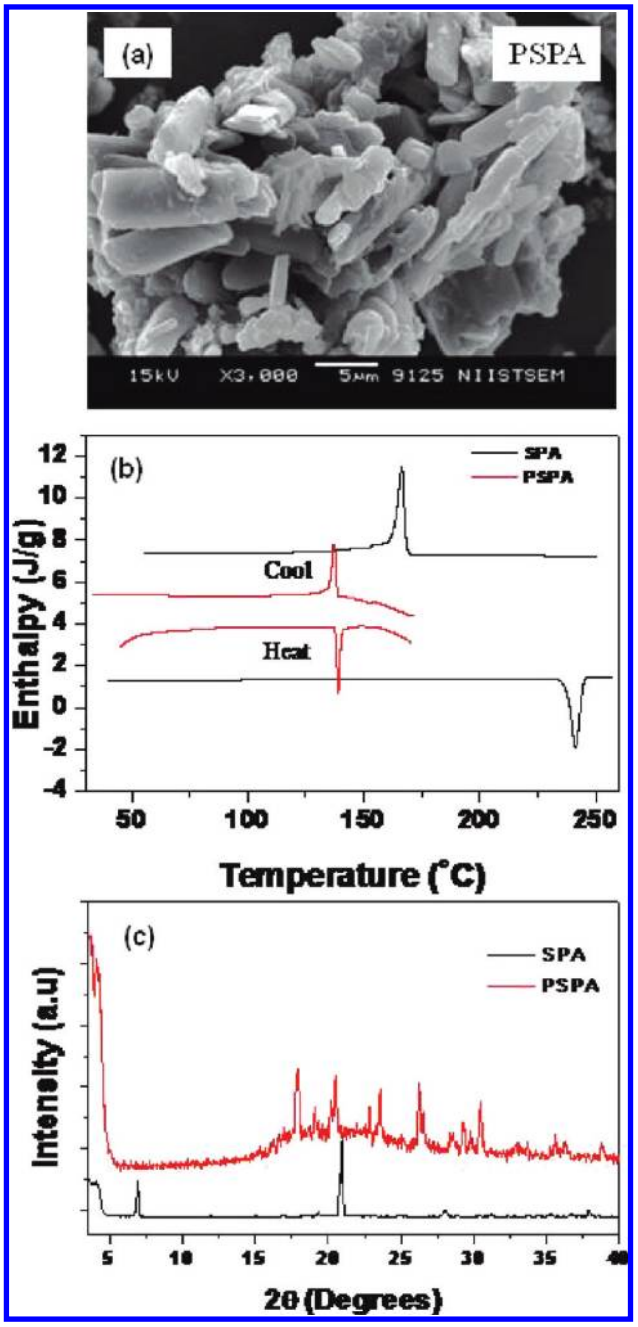

Figure 3. (a) SEM image of PSPA. (b) DSC thermograms of monomer and PSPA. (c) WXRD of monomer and PSPA.

confirmed the existence of the flakelike morphology (see the Supporting Information). The tendency for the formation of flakelike morphology in the present system is attributed to the self-doping nature of the polymers. The presence of sulfonic acid groups in the polymer chains induces strong interchain interactions for the formation of two-dimensional (2D) flakelike growth rather than 1D fibrous morphology. The enthalpy changes of the polymer on heating and cooling were recorded by using a differential scanning calorimeter (see Figure 3). The self-doped polymer showed melting and crystallization peaks at 139 °C (ΔH = 1.11 J/g) and 136 °C (ΔH = 1.08 J/g), respectively. The melting and crystallization peaks of the monomer (SPA) were obtained at 241.2 and 166.5 °C with ΔH of 30.7 and 27.1 J/g, respectively. The higher enthalpies of the transitions for the monomer compared to that of the polymer indicate that the monomer is highly crystalline compared to that of the resultant polymer structures. WXRD patterns of the polymers have showed sharp peaks at 2θ = 4.1° (d-spacing = 21.4 Å) with respect to highly ordered polymer structure.[31] PSPA showed sharp peaks at 2θ values from 17 to 30° with respect interchain interaction and aromatic $\pi-\pi$ interaction. Both DSC and WXRD analysis confirmed the existence of the highly crystalline nature of the self-doped polyaniline; however, the crystallinity of the monomer is much higher than that of the polymer. The thermal stabilities of the monomer, PSPA, and PSPANa were recorded by using a thermogravimetric analyzer under nitrogen flow (see the Supporting Information). The thermal stability of the materials increased in the following order: PSPA < SPA < PSPANa. Sulfonic acids are typically hygroscopic, and their storage and thermal stabilities are usually enhanced by converting them as sodium salts. In the present case also, as expected, the PSPANa is more stable compared to their acids (monomer and polymer). However, the slight increase in the thermal stability of SPA over PSPA could be correlated to the high crystalline of the monomer compared to the latter. $I-V$ plots for the polymers were measured using a four-probe conductivity meter, and the polymers showed a linear increase in voltage with an increase in current and followed typical ohmic behavior (see the Supporting Information). Four-probe conductivities of the doped and dedoped polymer samples were obtained as 1×10^{-3} and 6×10^{-5} S/cm, respectively, which match the values reported for N-substituted self-doped polyaniline samples.[35,36]

The polymers in both doped and dedoped forms possessed good solubility in water, and absorption spectra were recorded for various concentrations from 10^{-3} to 10^{-5} M (see the Supporting Information). Absorbance spectra of PSPA showed three absorption maxima at 305, 420, and 1040 nm corresponding to $\pi-\pi^*$, polaron$-\pi^*$, and $\pi-$bipolaron electronic transitions, respectively. The sample PSPANa showed two peaks at 300 and 640 nm corresponding to $\pi-\pi^*$ and exciton quinoid transitions, respectively.[22,40−42] The absorption maxima of the doped and dedoped polymer remained unchanged with the change in concentration. This clearly supports that the electronic structures of the self-doped and dedoped structures were stable in water irrespective of their concentration. The polymer possessed in-built sulfonic acid groups in the chain backbone, and therefore, the role of pH on the electronic transitions is very important to be analyzed. For this purpose, the concentration of PSPA was fixed as 1×10^{-3} M (pH = 3.2), and different concentrations of base NaOH or Na_2CO_3 were added to vary the pH from 3.2 to 12 (see Figure 4). Absorbance spectra show that, upon increasing the pH, the color of the polymer solutions transformed from the green to deep blue. This confirmed the change in the structure from emeraldine salt to emeraldine base with increase in the pH. The spectra showed major changes in the four different positions 305, 420, 640, and 1040 nm with respect to variation in the pH. On increasing the pH from 3.2 to 12.0, the polaron (at 420 nm) and bipolaron (1040 nm) vanish and a new peak at 640 nm corresponding to the quinoid ring appeared. The change in the absorbance $\Delta A = A_0 - A$, where A_0 and A correspond to the absorbance at initial and at particular pH (at 420, 640, and 1040 nm), was plotted against the pH of the solution (showed as inset in the Figure 4). The three plots of ΔA showed a sharp transition at pH = 8.6−9.6 with respect to their transformation in electronic structure from emeraldine base to

dx.doi.org/10.1021/la200047t |*Langmuir* 2011, 27, 6268–6278

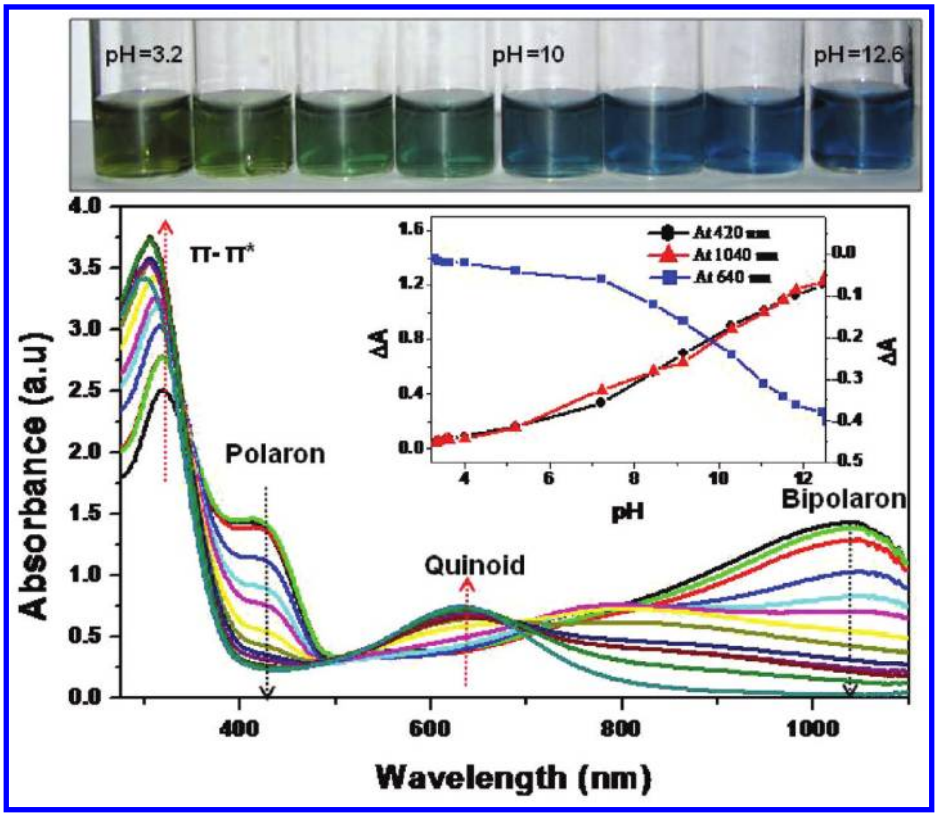

Figure 4. Absorption spectra of PSPA with increase in pH and photographs showing color changes with pH.

salt. The pH dependent absorbance studies revealed that the newly synthesized water-soluble N-substituted polyaniline provides a very sharp change in the color which is very attractive for the colorimetric sensing applications.

In order to trace the sensing ability of PSPANa, it was treated with various biomolecules (vitamins and amino acids) and dopants (mineral and organic acids) (see the Supporting Information). As expected, dopants such as camphorsulfonic acid (CSA) and HCl showed color change from blue to green with respect to the transformation of emeraldine base to salt. Biomolecules such as folic acid (vitamin B9), glycine, and lysine did not show any change due to weak protonation ability of their carboxylic functional groups. Interestingly, vitamin-C (ascorbic acid) and cysteine showed a sharp and unexpected change of color from the blue to colorless. To further understand the sharp color change followed by the addition of vitamin-C and cysteine into the self-doped polymer solution, a control experiment was carried out with unsusbtituted polyaniline emeraldine base (PANI-EB) (see the Supporting Information). The addition of vitamin-C into PANI-EB produced a green colored solution with respect to the formation emeraldine salt, whereas cysteine did not show any change. It suggests that the unusual color change from deep blue to colorless by the present polymer structure (PSPANa) was unique to the self-doped N-alkyl polyaniline and not for all emeraldine bases. Therefore, the new polymer design provides an opportunity for sensing of biomolecules such as vitamin-C and cysteine by simple colorimetric techniques. Further, the selectivities of cysteine and vitamin-C compared to other amino acids (more than 17 numbers) and other water-soluble vitamins were also tested (see the Supporting Information). The studies showed that the self-doped polymer possessed high selectivity only for vitamin-C and cysteine and not for other biomolecules.

The sensing action of vitamin-C and cysteine by PSPANa was quantitatively detected by absorption spectra using Job's plot and molar ratio method (see Figures 5 and 6, respectively). It is important to mention that sharp color change was noticed for vitamin-C in the sodium salts of polymers of NaOH and Na_2CO_3; however, the sensing for cysteine was found promising for polymer solutions obtained from Na_2CO_3 compared to NaOH. Upon adding vitamin-C (also cysteine), the color change was accompanied by disappearance of the peak at 640 nm (quinoid ring) with an increase in the absorbance at 300−320 nm. The spectral change at 640 nm was plotted against the mole fractions of the constituents, and this is shown in Figure 5 as inset. The stoichiometry of vitamin-C and cysteine with polymer was found as 3:2 and 4:1, respectively (the reason for the difference in stoichiometry difference is explained in the mechanism part below). In order to determine the association constant, the molar ratio method was executed by varying the concentration of the analyte (from 1×10^{-4} to 2×10^{-3} M of vitamin-C and cysteine) with fixed polymer concentration (3×10^{-4} M) (see Figure 6). The association constants were calculated using the Benensi−Hildebrand equation:

$$1/\Delta A = 1/[R^0]K\Delta\varepsilon_{RS}[S^0] + 1/[R^0]K\Delta\varepsilon_{RS}$$

where ΔA, $[R^0]$, $[S^0]$, and $\Delta\varepsilon_{RS}$ are the change in absorption, total receptor concentration, total substrate concentration, and molar absorptivities of RS ($\Delta\varepsilon_{RS} = \varepsilon_{RS-}\varepsilon_{R-}\varepsilon_S$), respectively.[43] The plot of $1/\Delta A$ versus 1/[vitamin-C] showed a straight line plot which suggests that the polymer + analyte followed the

dx.doi.org/10.1021/la200047t |*Langmuir* 2011, 27, 6268–6278

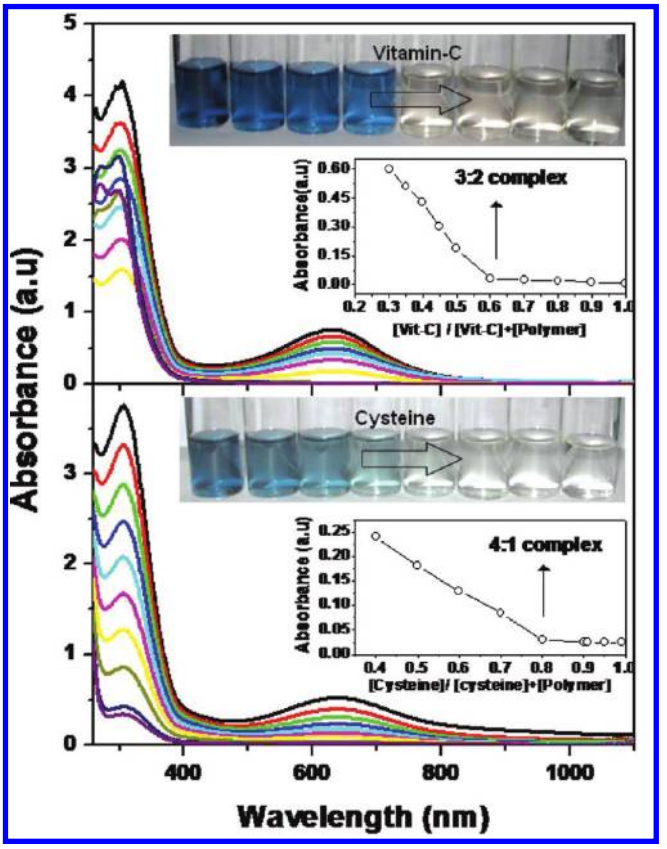

Figure 5. Change in the absorbance spectra of the polymers for the total concentration of [polymer + analyte] = 10^{-3} M in water with variation in the chemical compositions. Insets: Job's plots of the polymer + analyte complex.

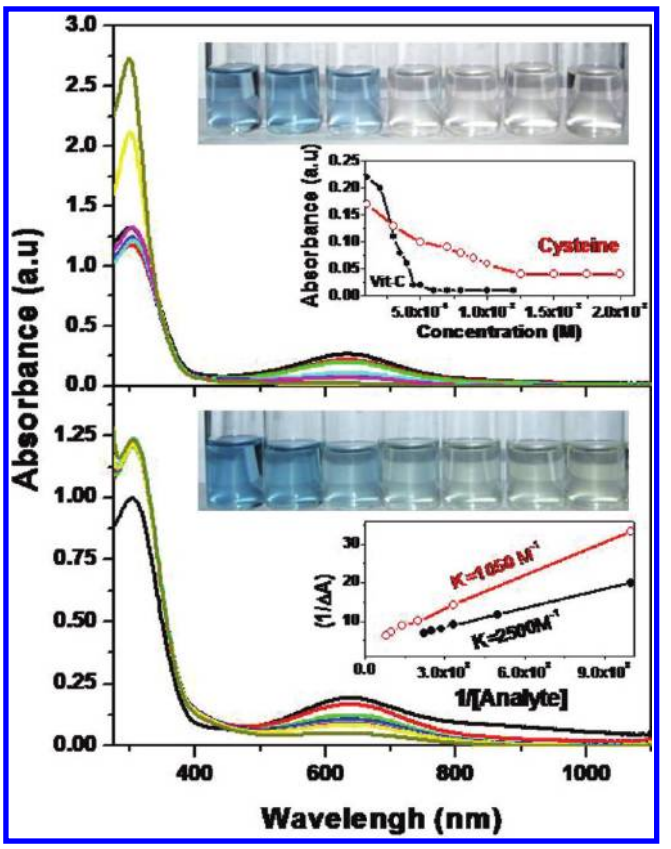

Figure 6. Absorbance spectra of the polymers upon addition of analytes into the fixed concentration of polymer, [polymer] = 3 × 10^{-4} M. Insets: molar ratio plots (top) and Benensi−Hildebrand plots (bottom) of the polymer + analyte complex.

Benensi−Hildebrand behavior. The binding constants (K) were calculated from the intercept/slope of the plots as 2.1 × 10^3 and 1.5 × 10^3 for vitamin-C and cysteine, respectively. The binding constants for vitamin-C and cysteine in the present case are comparable with those of other sensing substrate molecules such as fluorescence.[44] To study the colorimetric sensing ability in solid state form (for practical applications), a simple technique was constructed for the sensing action of vitamin-C and cysteine. A thin layer of surgical grade cotton was rolled over a plastic stick and dipped into the PSPANa solution to make a uniform blue coating (see Supporting Information). The blue color stick was stable for more than 2 days without color bleaching. A half-portion of blue stick was dipped to an analyte solution of vitamin-C, cysteine, HCl, and CSA. The blue color immediately changed into colorless for vitamin-C and cysteine, whereas green color appeared for HCl and CSA solution with respect to emeraldine salt formation. The detailed colorimetric studies in solution as well as in the solid support (on cotton) revealed that the present water-soluble polyaniline is unique and possessed blue to colorless sensing ability for biomolecules such as vitamin-C and cysteine in solution as well as in solid state.

The mechanism for the sensing of vitamin-C and cysteine is given in Figure 7. Chemical structures of self-doped polyaniline N-alkylated polyanilines are different from those of normal polyanilines, and they exist as the emeraldine salt (I) consisting of cation radicals of *p*-phenylenediamine.[45−47] Addition of base results in the formation of dedoped form of emeraldine base (II) consisting of dications of *p*-phenylenediimine. The dications were stabilized by counterion interaction of sulfonate anions attached in the adjacent polymer chains via electrostatic self-assembly (see Figure 7).[28,41,42] Vitamin-C (ascorbic acid) is a dibasic acid for proton transfer to bases and also good reducing agent via transfer of electrons. In the presence of dedoped polymer, vitamin-C undergoes redox reaction to produce dehydroascorbic acid and gives away $2e^-$ and $2H^+$. Cysteine is another important reducing biomolecule which undergoes self-oxidation to produce cystine with disulfide linkage and give away $2e^-$ and $2H^+$. Therefore, the reaction of vitamin-C and cysteine with N-alkyl polyaniline backbone is a typical example of the redox process from the analyte to substrate. The addition of vitamin-C (or cysteine) into polymer induces the following changes: (i) protonation of sodium salts of sulfonic acids in the alkyl side chain which further dissociates the electrostatic interaction between SO_3^- and Ph−N^+ cations, (ii) transfer of the two electrons from analyte to the dications of *p*-phenylenediimine units in the polymer and convert the polymer chain into completely reduced form, that is, leucoemeraldine base form. As a net result of the proton and electron transfer from vitamin-C (also cysteine) to PSPANa (blue color), the color of the polymer solution changes from blue to colorless. Since the kinetics is very fast (observed in the range of k_{ET} = 4 × 10^6 s^{-1}),[48] it accompanies the color change instantaneously for colorimetric detection by naked eye. The higher stoichiometry (4:1, in moles) of cysteine could be explained from the mode of chemical reaction it undergoes during the sensing process (see Figure 7). Two cysteine molecules are oxidized to form one cystine molecule to give $2H^+$

dx.doi.org/10.1021/la200047t |*Langmuir* 2011, 27, 6268–6278

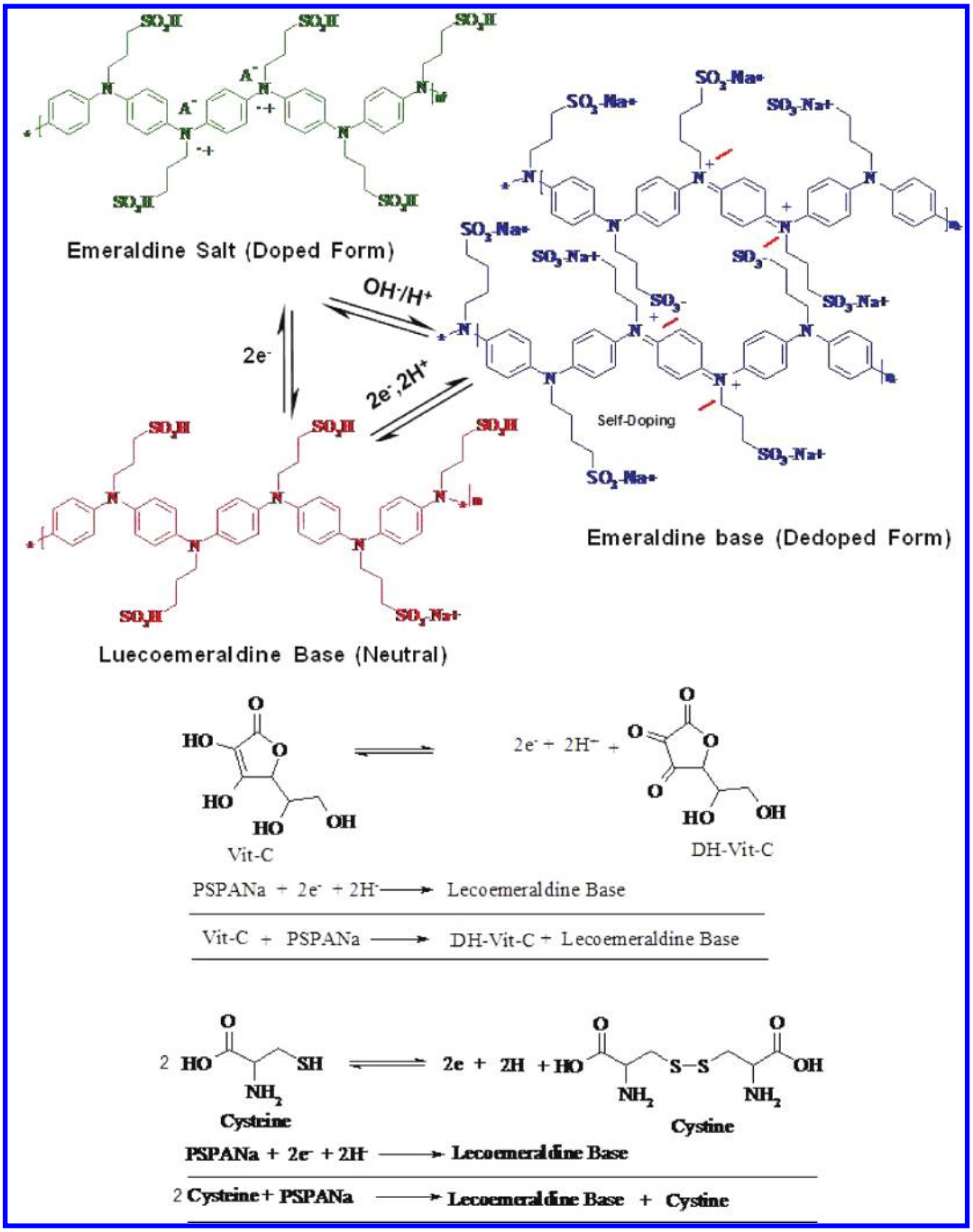

Figure 7. Mechanism of colorimetric sensing in self-doped N-substituted polyaniline with analytes.

and $2e^-$. On the other hand, in the case of vitamin-C, each molecule undergoes oxidation to dehydroascorbic acid (DHAA) and $2H^+$ and $2e^-$. This further reflects the high detecting ability of vitamin-C and higher association constant compared to that of cysteine (see insets in Figure 5). To understand the ET process, the oxidation and reduction potential of PSPANa and its complexes with vitamin-C and cysteine were determined by cyclic voltammetry in water using glassy carbon working electrode (see Figure 8). All samples are recorded in the range of +1.2 to −1.2 V at a scan rate of 50 mV/s. Bases (NaOH and Na_2CO_3 in water) act as electrolytes to retain the same experimental procedure used for sensing (little excess of the analyte is used to stabilize the signal in the CV). The cyclic voltammogram of PSPANa showed an anodic oxidation peak at 0.46 mV in the anodic sweep and a reversible reduction peak at −0.21 V in the negative cathodic region.[49,50] Under the same sweeping conditions, the oxidation potential of vitamin-C and cysteine were found as 0.11 and 0.54 V, respectively (see the Supporting Information). Cyclic voltammograms of vitamin-C + PSPANa and cysteine + PSPANa complexes showed complete disappearance of the cathodic peak at −0.21 V. The disappearance of the cathodic peak at −0.21 V upon the addition of analytes (vitamin-C and cysteine) revealed the electron transfer from the analyte to the polymer backbone and supports the mechanism proposed in Figure 7. To further investigate the electron transfer process on the conductivity of the samples in the solid state, a 10 mm diameter pellet of the

dx.doi.org/10.1021/la200047t |*Langmuir* 2011, 27, 6268–6278

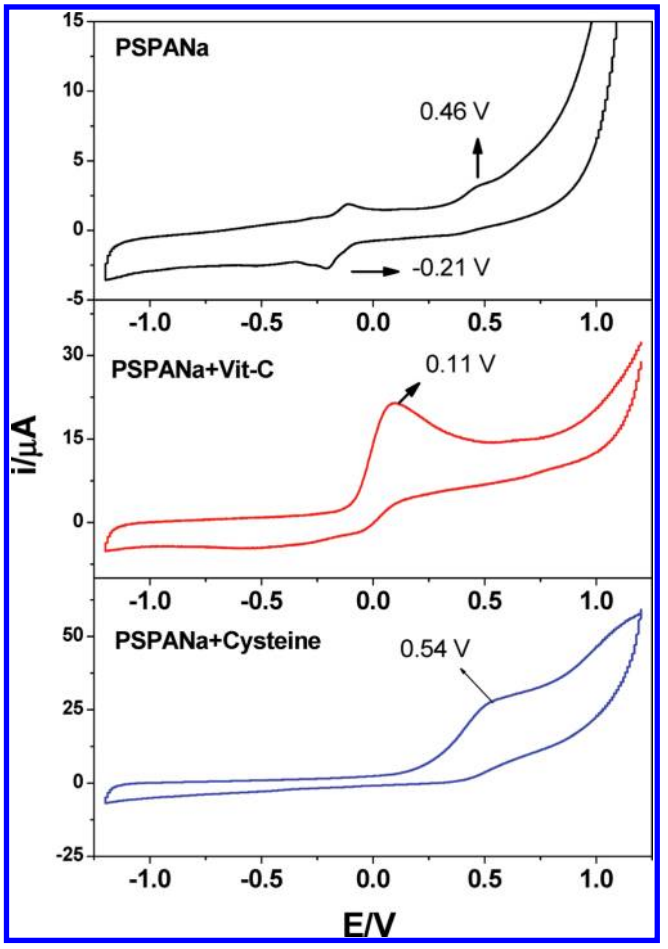

Figure 8. Cyclic voltammograms of PSPANa, PSPANa + vitamin-C, and PSPA + cysteine.

PSPANa was made and subjected to sensing studies. The blue color pellet was dipped into vitamin-C (or cysteine) solution, and the resultant pellet was subjected to four-probe conductivity measurements. The conductivity of the PSPANa pellet changed from 6×10^{-5} to 2.5×10^{-6} and 1.5×10^{-6} S/cm followed by dipping in vitamin-C and cysteine, respectively. The decrease in the conductivity values confirmed the formation of reduced leucoemeraldine base form through electron transfer process as shown in Figure 7. It confirmed that the water-soluble self-doped polyaniline is a very unique and efficient sensor material for detecting biomolecules such as vitamin-C and cysteine via electron transfer process.

Electron transfer is a short-range order process typically occurred in a closed vicinity of the electron donor and acceptor species. In biological systems, such as flavoenzymes, the electron transfer is efficient because the protein folding creates close packing of the reaction site for electron transfer between donors and acceptors.[51−55] In synthetic molecules, close contact between donor and acceptor units is achieved either via covalent linkages or in the coordinated crystal structures. It is very surprising to notice that, in the present case, the ET process was efficient between the conducting polymers with analytes (vitamin-c or cysteine) which are not chemically interconnected together. Therefore, it is very important to trace the molecular interactions between vitamin-C (and cysteine) with PSPANa to understand the ET process. In order to trace the molecular

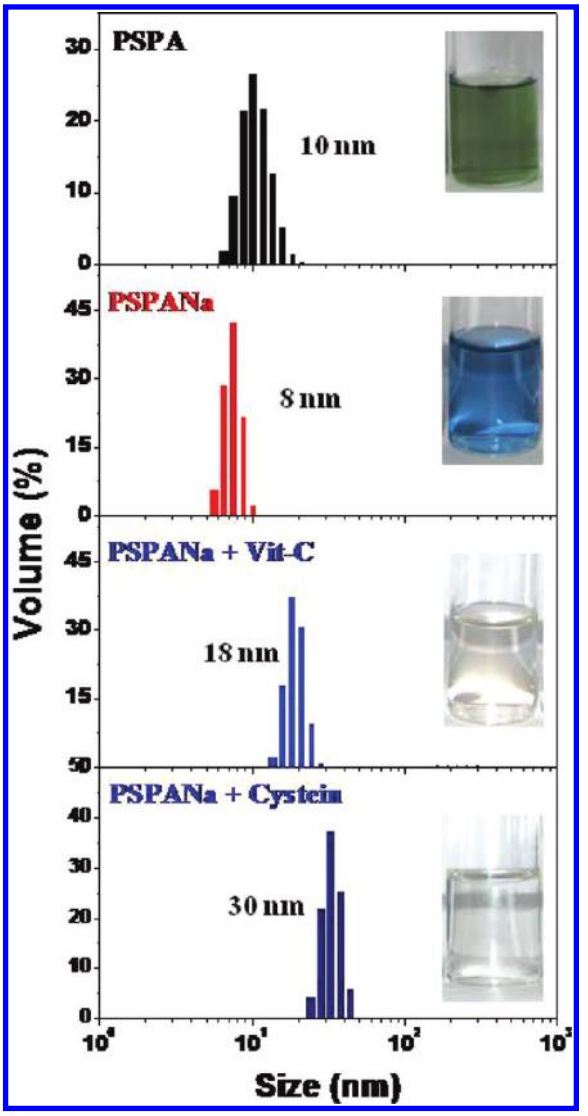

Figure 9. DLS histograms of the PSPA, PSPANa, PSPA + vitamin-C, and PSPA + cysteine in water at 25 °C. [Polymer] = 4×10^{-4} M and [analyte] = 1×10^{-3} M.

interactions, the polymer solutions in doped (PSPA) and dedoped (PSPANa) forms were subjected to dynamic light scattering (DLS) coupled with zeta potential measurements. DLS histograms of PSPA, PSPANa, PSPANa + vitamin-C, and PSPANa + cysteine are shown in Figure 9. Polymer samples in doped and dedoped forms showed uniform distribution of aggregates with average sizes of 8 and 10 nm, respectively. DLS analysis was also done for a stored polymer solution over a period of 1 week; the polymer did not phase separate, and the results were almost reproducible. The polymers possessed typical amphiphilic structure in which the aromatic backbone and alkyl sulfonic acid groups act as hydrophobic and hydrophilic parts. Nanomicellar aggregates form a core−shell architecture in which the hydrophilic sulfonic acid part is kept outside facing the aqueous environment and the polyaniline backbone provides the hydrophobic core. Upon dedpoing the PSPA with sodium hydroxide, the outer sulfonic acid groups converted into sodium sulfonate and the polyaniline backbone became quinonid; however, the hydrophilicity of the core and outer shell was retained. Therefore, during chemical doping/dedoping processes, the

dx.doi.org/10.1021/la200047t |*Langmuir* 2011, 27, 6268–6278

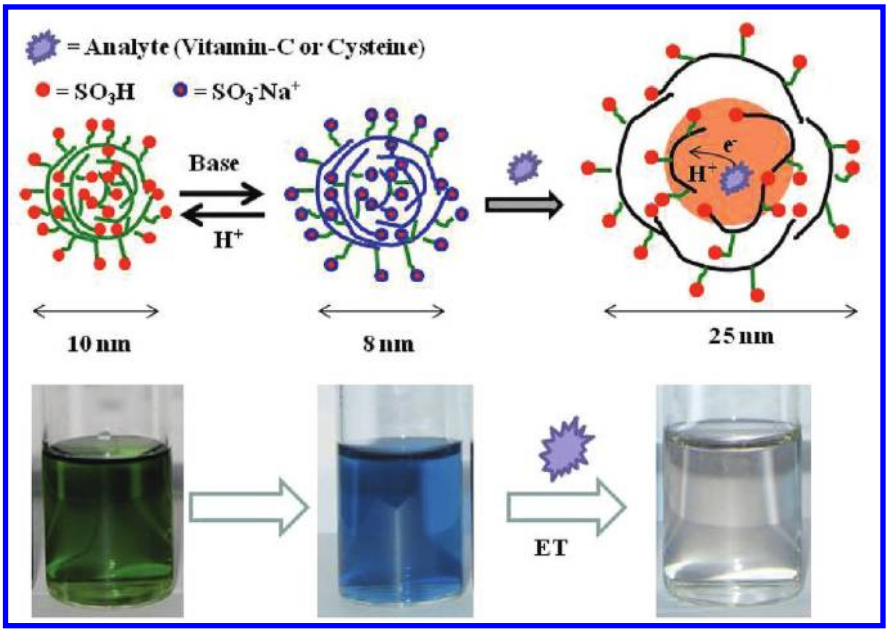

Figure 10. Schematic model for the colorimetric sensing via ET process in the polymer nanoaggregates.

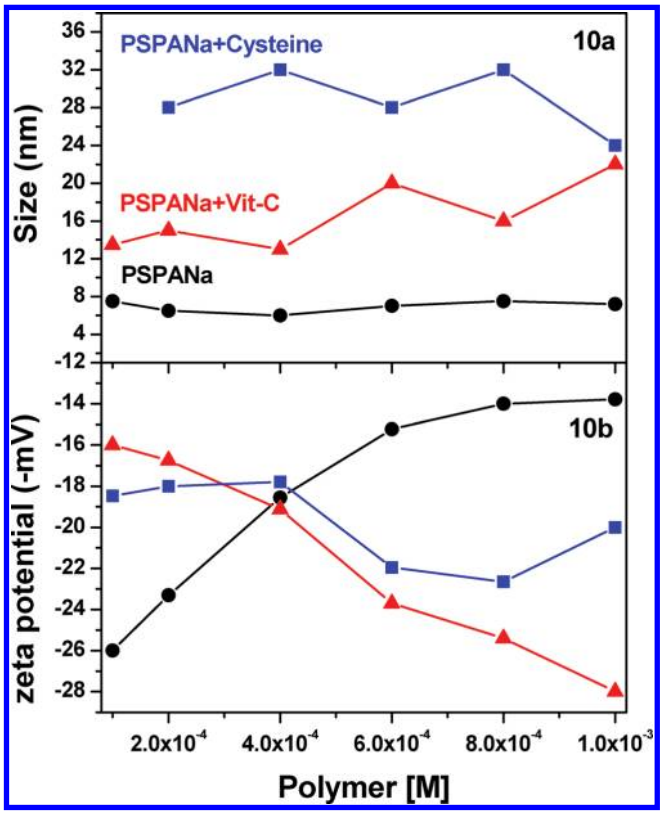

Figure 11. Size and zeta potentials of PSPANa, PSPANa + vitamin-C, and PSPANa + cysteine at various polymer concentrations for fixed [analyte] = 1×10^{-3} M.

polymer chains were retained in the nanoaggregate form without affecting the hydrophilic/hydrophobic nature of the aggregates. A schematic model for the polymer nanoaggregates is shown in Figure 10.

Zeta potential measurement is very important tool for understanding the solution dynamic of charged particles or aggregates, like the doped and dedoped polymers in the presence case. Electrically charged species tend to move under the influence of an electric field, and the electrical potential at the surface of the sphere of radius a and carrying charge q is $\zeta = q/4\pi\varepsilon a$, where ζ and ε are zeta potential and permittivity of the medium in which they are immersed, respectively.[56] The effect of concentration on the size of the micellar aggregates and their zeta potential are shown in Figure 11 (for DLS histograms, see the Supporting Information). The size of the nanoaggregates in PSPANa was less influenced by concentration variation, and the values were found in the range of 10 ± 2 and 8.0 ± 2 nm for both doped and dedoped structures, respectively. The aggregate sizes of the PSPANa + vitamin-C and PSPANa + cysteine complexes were found to be much higher than that of their homopolymer aggregates. The addition of analytes into the polymer solution increases the sizes of aggregates from 10 to 20 and 30 nm for vitamin-C and cysteine, respectively. However, we need more experimental evidence to confirm the occupancy of analyte in the hydrophobic cavity of the nanoaggregates. The analytes are typical organic molecules, and they can preferentially occupy the hydrophobic cavity provided in the nanoaggregates, and these phenomena attributed to the increase in the size of the aggregates. The zeta potential of the polymer nanoaggregates possessed negative charges; however, their magnitude varies with the type of structure. All three plots of zeta potential versus concentration showed a nonlinear trend with a break point at 4.0×10^{-4} M, which is very close to the critical micellar concentration (CMC) of these nanoaggregates. Since polymer chains possessed long-range chain interactions, unlike in the case of small molecule surfactants, it may contain critical association well below the CMC. Nevertheless, the detailed DLS and zeta potential studies confirmed that the addition of vitamin-C or cysteine did not destabilize the polymer nanoaggregate and the aggregates are stable for a wider concentration range for the detection process. Thus, the newly synthesized self-organized nanoaggregates provide reaction sites in which electron transfer occurred between the analyte and polyaniline backbone for colorimetric sensing of vitamin-C and cysteine.

dx.doi.org/10.1021/la200047t |*Langmuir* 2011, 27, 6268–6278

CONCLUSION

In conclusion, a water-soluble self-doped polyaniline was synthesized and successfully utilized as substrate for detection of biomolecules such as vitamin-C and cysteine via electron transfer in nanoaggregates. The main outcomes of the present investigation are as follows: (i) *N*-propylsulfonic acid aniline monomer was synthesized via ring-opening of sultone with aniline, which was further polymerized via chemical oxidative route to produce completely water-soluble polyaniline; (ii) the structures of the polymers in doped and dedoped forms were characterized by both ^{1}H and ^{13}C NMR, and the molecular weights were determined by viscosity and MALDI-TOF techniques; (iii) pH dependent absorbance studies revealed that the newly synthesized water-soluble N-substituted polyaniline provides very sharp color change which is very attractive for the colorimetric sensing applications; (iv) various dopants such as camphorsulfonic acid (also HCl) showed expected color change from blue to green with respect to the transformation of emeraldine base to its salt; (v) the unusual color change from deep blue to colorless by PSPANa was unique to the self-doped N-alkyl polyaniline structure and provides new opportunity for sensing of biomolecules such as vitamin-C and cysteine by simple colorimetric techniques; (vi) Job's plots for vitamin-C and cysteine established the stoichiometric composition of vitamin-C and cysteine with polymer as 3:2 and 4:1, respectively; (vii) the binding constants were determined by molar ratio method using Benensi−Hildebrand plots, and $K = 2.1 \times 10^3$ and 1.5×10^3 M^{-1} were obtained for vitamin-C and cysteine, respectively; (viii) vitamin-C gives away $2H^+$ and $2e^-$ in the presence of dedoped polymer which were donated to sulfonate anions and dications of the *p*-phenylenediimine backbone; (ix) cysteine undergoes self-oxidation to produce cystine with disulfide linkage and give away $2e^-$ and $2H^+$ which were donated to polyaniline as in the case of vitamin-C; (x) cyclic voltammetry studies confirmed the electron transfer from the analyte to polymer with disappearance of the cathodic peak at −0.21 V in the polymers upon the addition of analytes (vitamin-C and cysteine); and (xi) dynamic light scattering with zeta potential measurements confirmed the existence of 8−10 nm aggregates of polymer self-assembly in water. The analytes are typical organic molecules and preferentially occupied the hydrophobic cavity provided in the nanoaggregates in which the efficient proton and electron transfer occurred between the analyte and polyaniline backbone for colorimetric sensing process. In a nutshell, the electron transfer process is successfully exploited in nanomicellar aggregates of N-substituted polyaniline for the detection of biomolecules such as vitamin-C and cysteine.

ASSOCIATED CONTENT

Supporting Information. ^{13}C NMR of the monomer (SPA), PSPA, and PSPANa; HR-MS(FAB) mass of the monomer (SPA); FT-IR of the monomer (SPA), PSPA, and PSPANa; MALDI-TOF-TOF of the monomer PSPA; SEM and TEM images of PSPA and PSPANa; TGA profile of monomer (SPA) and PSPA; temperature dependent *I*−*V* plots of the PSPA; concentration dependent absorption spectra of the PSPA and PSPANa at 30 °C; colorimetric sensing of the vitamin-C and cysteine using PSPANa in solution and solid supported state; photographs of vials showing color changes in PANI-EB on addition of vitamin-C and cysteine as a control experiment; photographs of the vials showing the selectivity of L-cysteine over other L-amino acids; photographs showing selectivity of vitamin-C by PSPANa and absorption spectra with addition of different water-soluble vitamins; cyclic voltammetry of vitamin-C and cyteine. This material is available free of charge via the Internet at http://pubs.acs.org.

AUTHOR INFORMATION

Corresponding Author

*E-mail: jayakannan@iiserpune.ac.in. Fax: 0091-20-25898022.

ACKNOWLEDGMENT

We thank the Department of Science and Technology, New Delhi, India under the NSTI Programme-SR/S5/NM-06/2007 and SR-NM/NS-42/2009 for financial support. M.J.A. thanks UGC-New Delhi, India for Senior Research Fellowship (SRF).

REFERENCES

(1) McQuade, D. T.; Pullen, A. E.; Swager, T. M. *Chem. Rev.* **2000**, *100*, 2537–2574.
(2) Li, D.; Haung, J.; Kaner, R. B. *Acc. Chem . Res.* **2009**, *42*, 135–145.
(3) Huang, J.; Virji, S.; Weiller, B, H.; Kaner, R. B. *Chem.—Eur. J.* **2004**, *10*, 1314–1319.
(4) Janata, J.; Josowich, M. *Nat. Mater.* **2003**, *2*, 19–24.
(5) Feng, F.; Tang, Y.; He, F.; Yu, M.; Duan, X.; Wang, S.; Li, Y.; Zhu, D. *Adv. Mater.* **2007**, *19*, 3490–3495.
(6) Duan, X.; Liu, L.; Feng, F.; Wang, S. *Acc. Chem. Res.* **2010**, *43*, 260–270.
(7) Jiang, G.; Susha, A. S.; Lutich, A. A.; Stefani, F. D.; Feldmann, J.; Rogach, A. L. *ACS Nano* **2009**, *3*, 4127–4131.
(8) Feng, F.; Liu, F.; Wang, S. *Nat. Protoc.* **2010**, *5*, 1255.
(9) Bossi, A.; Piletsky, S. A.; Piletska, E. V.; Righetti., P. G.; Turner, A. P. F. *Anal. Chem.* **2000**, *72*, 4296–4300.
(10) Ali, S. R.; Parajuli, R. R.; Ma, Y.; Balogun, Y.; He, H. *J. Phys. Chem. B* **2007**, *111*, 12275–12281.
(11) Shoji, E.; Freund, M. S. *J. Am. Chem. Soc.* **2001**, *123*, 3383–3384.
(12) Ali, S. R.; Ma, Y.; Parajuli, R. R.; Balogun, Y.; Lai, W. Y. C.; He, H. *Anal. Chem.* **2007**, *79*, 2583–2587.
(13) Jureviciute, I.; Brazdiuviene, K.; Bernotaite, L.; Salkus, B.; Malinauskas, A. *Sens. Actuators, B* **2005**, *107*, 716–721.
(14) Jiang, Y.; Wang, A.; Kan, J. *Sens. Actuators, B* **2007**, *124*, 529–534.
(15) Korcherginsky, N. M.; Wang, Z. *J. Electroanal. Chem.* **2007**, *611*, 162–168.
(16) Gerard, M.; Chaubey, A.; Malhotra, B. D. *Biosens. Bioelectron.* **2002**, *17*, 345–359.
(17) Andreu, Y.; Marcos, S. D.; Castillo, J. R.; Galban, J. *Talanta* **2005**, *65*, 1045–1051.
(18) Virji, S.; Kaner, R. B.; Weiller, B. H. *J. Phys. Chem. B* **2006**, *110*, 22266–22270.
(19) Komsiyaska, L.; Tsakova, V. *Electroanalysis* **2006**, *8*, 807–813.
(20) Casella, I. G.; Guascito, M. R. *Electroanalysis* **1997**, *9*, 1381–1386.
(21) Zhang, L. *J. Solid State Electrchem.* **2007**, *11*, 365–371.
(22) Chen, S.-A.; Hwang, G.-W. *J. Am. Chem. Soc.* **1995**, *117*, 10055–10062.
(23) Lin, H. K.; Chen, S.-A. *Macromolecules* **2000**, *33*, 8117–8118.
(24) Malinauskas, A. *J. Power Sources* **2004**, *126*, 214–220.
(25) Nguyen, M. T.; Kasi, P.; Miller, J. L.; Daiz, A. F. *Macromolecules* **1994**, *27*, 3625–3631.
(26) Sivakumar, C.; Vasudevan, T.; Gopalan, A. *Ind. Eng. Chem. Res.* **2001**, *40*, 40–51.
(27) Freund, M. S.; Deore, B. A. *Self-Doped Conducting Polymers*; John Wiley & Sons Ltd.: West Sussex, England, 2007.

(28) Chen, S. A.; Hwang, G.-W. *J. Am. Chem. Soc.* **1994**, *116*, 7939–7940.
(29) +Yue, J.; Wang, Z, H.; Kromack, K. R.; Epstein, A. J.; Macdiarmid, A. G. *J. Am. Chem. Soc.* **1991**, *113*, 2665–2671.
(30) (a) Anilkumar, P.; Jayakannan, M. *Langmuir* **2008**, *24*, 9754–9762. (b) Antony, M. J.; Jayakannan, M. *J. Phys. Chem. B* **2007**, *111*, 12772. (c) Antony, M. J.; Jayakannan, M. *J. Polym. Sci., Part B: Polym. Phys.* **2009**, *47*, 830. (d) Antony, M. J.; Jayakannan, M. *J. Phys. Chem. B* **2010**, *114*, 1314–1324. (e) Anilkumar, P.; Jayakannan, M. *Langmuir* **2006**, *22*, 5952. (f) Anilkumar, P.; Jayakannan, M. *J. Phys. Chem. B* **2010**, *114*, 728–736. (g) Anilkumar, P.; Jayakannan, M. *J. Phys. Chem. B* **2009**, *113*, 11614–11624. (h) Anilkumar, P.; Jayakannan, M. *J. Phys. Chem. B* **2010**, *114*, 728–736.
(31) Lou, X.; Zhang, L.; Qin, J.; Zhen, L. *Langmuir* **2010**, *26*, 1566–1569.
(32) Miller., S. *Anal. Chem.* **2010**, *82*, 1570.
(33) Balamurugan, A.; Reddy, M. P.; Jayakannan, M. *J. Phys. Chem. B* **2010**, *113*, 14128–14138.
(34) Sandberg, M. O.; Nagao, O.; Wu, Z.; Matsushita, M. M.; Sugawara, T. *Chem. Commun.* **2008**, 3738–3740.
(35) Wei, Y.; Hsueh, K. F.; Jang, G.-Y. *Macromolecules* **1994**, *27*, 518–525.
(36) Moon, D.-K.; Ezuka, M.; Maruyama, T; Osakada, Y. *Macromolecules* **1993**, *26*, 364–369.
(37) Mu, S.; Yang, Y. *J. Phys. Chem. B* **2008**, *112*, 11558–11563.
(38) Zhang, J.; Shan, D.; Mu, S. *J. Polym. Sci., Part A: Polym. Chem.* **2005**, *43*, 1767–1777.
(39) Zhang, J.; Shan, D.; Mu, S. *Polymer* **2007**, *48*, 1269–1275.
(40) Cataldo, F.; Maltese, P. *Eur. Polym. J.* **2002**, *38*, 1791–1803.
(41) Nabid, M. R.; Entezami, A. A. *Polym. Adv. Technol.* **2005**, *16*, 305–309.
(42) Yuan, G.-L.; Kuramato, N. *Macromolecules* **2003**, *36*, 7939–7945.
(43) Atood, J. L.; Davies, J. E. D.; Macnicol, D. D.; Vogtle, F.; Lehn, J. M.; Suslick, K. S. *Comprehensive supramolecular chemistry*; Pergamon: Oxford, U.K., 1996; Vol. 8, pp 439−441.
(44) Zou, W.; Yue, P.; Lin, L.; He, M.; Zhou, Z.; Lonial, S.; Khuri, F, R.; Wang, B.; Sun, S.-Y. *Clin. Cancer Res.* **2006**, *12*, 273–280.
(45) Kim, E.; Lee, M.; Rhee, S.-H. *Synth. Met.* **1995**, *69*, 101–104.
(46) Lindfors, T.; Ivaska, A. *J. Electroanal. Chem.* **2002**, *535*, 65–74.
(47) Bergeron, J.; Chevaliar, J.-W.; Dao, L. H. *J. Chem. Soc. Chem. Commun.* **1990**, 180–182.
(48) Young, E. R.; Rosenthal, J.; Hodgkiss, J. M.; Nocera, D. G. *J. Am. Chem. Soc.* **2009**, *131*, 7678–7684.
(49) Heras, J. Y.; Giacobone, A. F. F.; Battaglini, F. *Talanta* **2007**, *71*, 1684–1689.
(50) Krishnamoorthy, K.; Contractor, A. Q.; Kumar, A. *Chem. Commun.* **2001**, 240–241.
(51) Kurreck, H.; Boch, M.; Bretz, N.; Elsner, M.; Kraus, H.; Lubitz, W.; Muller, F.; Giessler, J.; Kroneck, P. M. H. *J. Am. Chem. Soc.* **1984**, *106*, 734–746.
(52) Schiffer, S. H. *Acc. Chem. Res.* **2006**, *39*, 93–100.
(53) Huynh, M. H.; Meyer, T. J. *Chem. Rev.* **2007**, *107*, 5004–5064.
(54) Schiffer, S.-H.; Soudackov, A. V. *J. Phys. Chem. B* **2008**, *112*, 14108–14123.
(55) Shafirovich, V.; Geacintov, N. E. *Top. Curr. Chem.* **2004**, *237*, 129–157.
(56) Evert, D. H. *Basic Principles of Colloid Science*; Royal Society of Chemistry: London, 1988.